Secrecy Throughput of ANECE Assisted Transmission of Information in Finite Blocklength

Ishmam Zabir, *Student Member, IEEE,* Ananthram Swami, *Fellow, IEEE,* Yingbo Hua, *Fellow, IEEE*

***Abstract*—Anti-eavesdropping channel estimation (ANECE) among two or more cooperative full-duplex radio devices allows these devices to obtain their receive channel state information (CSI) with respect to each other but at the same time prevents eavesdropper (Eve) from obtaining any consistent estimate of its receive CSI, which improves the secrecy of subsequent transmission of information between the devices. This paper presents an analysis of secrecy throughput of ANECE assisted transmission of information between such single-antenna devices against Eve with multiple antennas. The analysis is based on finite blocklength coding and assumes that Eve applies a standard approach for information detection. Easy-to-compute analytical expressions of secrecy throughput in terms of various controllable parameters are obtained. Numerical results are discussed.**

***Index Terms*—Finite blocklength, physical layer security, secrecy throughput, full-duplex, ultra-reliable low-latency communications.**

I. Introduction

Anti-eavesdropping channel estimation (ANECE) was proposed in [1] to allow two or more cooperative full-duplex radio devices to obtain consistent estimates of their receive channel state information (CSI) but at the same time it disables eavesdropper (Eve) from obtaining any consistent estimate of its receive CSI. This property of ANECE is useful to maintain a non-zero secrecy rate of the subsequent transmissions of information between these devices against Eve with any number of antennas [2].

In this paper, we provide an analysis of an averaged secrecy throughput (AST) of ANECE assisted transmission of information from one single-antenna device to another against Eve with multiple antennas. This analysis assumes that Eve applies a standard method for information detection.

Furthermore, we consider a relatively short or often called finite blocklength (FBL) transmission of information between devices, which is important for applications such as Internet-of-Things (IoT) [4]-[5]. Prior AST analyses of FBL transmissions are available in [6]-[8] where the CSI anywhere is assumed to be known everywhere. In particular, Eve's receive CSI is assumed to be known to Eve. In the ANECE assisted case, Eve no longer knows its receive CSI perfectly, which makes the prior results inapplicable.

This work was supported in part by the Army Research Office under Grant Number W911NF-17-1-0581 and the Department of Defense under W911NF-19-S-0013. The views and conclusions contained in this document are those of the authors. I. Zabir and Y. Hua (*corresponding author*) are with Department of Electrical and Computer Engineering, University of California, Riverside, CA 92521, USA (email: izabi001@ucr.edu; yhua@ee.ucr.edu.). A. Swami is with US Army Research Laboratory, USA (email: ananthram.swami.civ@army.mil).

However, we will apply some of the techniques in [9]-[10] to the ANECE assisted case. We also assume that the forced channel estimation error at Eve (due to ANECE) is only treated by Eve as a source of additional noise at Eve. In other words, Eve does not apply advanced methods such as blind detection [2] to mitigate the effect of ANECE.

In section II, we provide details of system model and briefly describe ANECE. Also derived in that section are the effects of ANECE pilots, the SNRs at Bob and Eve, and the basic expression for AST. In section III, we provide a detailed analysis of AST in order to obtain easy-to-compute expressions of AST. In section IV, we illustrate the effects of various parameters on AST. Concluding remarks are provided in section V.

II. System Model

We consider N single-antenna cooperative full-duplex devices/users subject to a covert/passive eavesdropper (Eve) with N_E antennas, at an unknown location. To combat eavesdropping, all users apply anti-eavesdropping channel estimation (ANECE) [1] as follows. In phase 1, all users transmit ANECE pilots simultaneously, where the pilot transmitted by user j over n_1 time slots is denoted by $p_j(k)$ with $k = 1, \cdots, n_1$, and $n_1 \geq N-1$. The pilots can be also represented by $\mathbf{p}_j = [p_j(1), .., p_j(n_1)]^T, \ \forall j$ and $\mathbf{P} = [\mathbf{p}_1, .., \mathbf{p}_N]^T$. For ANECE, we need $rank(\mathbf{P}) = rank(\mathbf{P}_{(i)}) = N-1, \forall i$, where $\mathbf{P}_{(i)}$ results from removing the ith row of $\mathbf{P}$. The reduced-rank condition of $\mathbf{P}$ and the full-rank condition of $\mathbf{P}_{(i)}$ $\forall i$ are the required properties of ANECE pilots. An example of such a pilot matrix is $\mathbf{P} = \mathbf{DQV}$ where $\mathbf{D}$ is a diagonal matrix for power control, $\mathbf{Q}$ is a $N \times (N-1)$ submatrix of the $N \times N$ discrete Fourier transform (DFT) matrix and $\mathbf{V}$ is a $(N-1) \times n_1$ matrix satisfying $\mathbf{V}\mathbf{V}^H = \mathbf{I}_{N-1}$, e.g., see [1], [3]. We will assume that each row of $\mathbf{P}$ has squared norm equal to $P_1 n_1$.

In phase 1, the $n_1 \times 1$ signal vector received by user i is

$$\mathbf{y}_i = \sum_{j \neq i}^{N} h_{i,j}\mathbf{p}_j + \mathbf{n}_i = \mathbf{P}_{(i)}^T \mathbf{h}_{(i)} + \mathbf{n}_i, \tag{1}$$

where $h_{i,j}$ is the complex channel gain from user j to user i, $\mathbf{h}_{(i)}$ is the vertical stack of $h_{i,j}$ for all $j \neq i$, and $\mathbf{n}_i$ is the background noise (including residual self-interference of the full-duplex user). We assume that $h_{i,j}$ equals $h_{j,i}$ (reciprocal

channels), $h_{i,j}$ is $\mathcal{CN}(0,\sigma_{i,j}^2)$, and $\mathbf{n}_i$ is $\mathcal{CN}(\mathbf{0},\mathbf{I})$. The $N_E \times n_1$ signal matrix received by Eve can be expressed as

$$\mathbf{Y}_E = \sum_{i=1}^{N} \mathbf{h}_{E,i}\mathbf{p}_i^T + \mathbf{N}_E = \mathbf{H}_E\mathbf{P} + \mathbf{N}_E, \tag{2}$$

where $\mathbf{h}_{E,i}$ is the channel vector from user i to Eve, and $\mathbf{H}_E$ (Eve's receive channel matrix or CSI) is the horizontal stack of $\mathbf{h}_{E,i}$ for all i.

As shown next, the ANECE pilots allow every user to have a consistent estimate of their channel gains but do not allow Eve to have a consistent estimate of Eve's receive channel matrix.

A. Effect of the ANECE Pilots

We will consider minimum-mean-squared-error (MMSE) channel estimation at users and Eve. Let $\mathbf{K}_{\mathbf{x},\mathbf{y}} = \mathcal{E}[\mathbf{x}\mathbf{y}^H]$ denote the covariance matrix between two zero-mean random vectors $\mathbf{x}$ and $\mathbf{y}$, and let $\mathbf{K}_{\mathbf{x}} = \mathbf{K}_{\mathbf{x},\mathbf{x}}$. Then the MMSE estimate of the channel vector $\mathbf{h}_{(i)}$ at user i is

$$\begin{aligned}\hat{\mathbf{h}}_{(i)} &= \mathbf{K}_{\mathbf{h}_{(i)},\mathbf{y}_i}\mathbf{K}_{\mathbf{y}_i}^{-1}\mathbf{y}_i \\ &= \mathbf{\Sigma}_{(i)}^2\mathbf{P}_{(i)}^*(\mathbf{I}_{n_1} + \mathbf{P}_{(i)}^T\mathbf{\Sigma}_{(i)}^2\mathbf{P}_{(i)}^*)^{-1}\mathbf{y}_i \\ &= \mathbf{\Sigma}_{(i)}\big(\mathbf{I}_{N-1} + \mathbf{\Sigma}_{(i)}\mathbf{P}_{(i)}^*\mathbf{P}_{(i)}^T\mathbf{\Sigma}_{(i)}\big)^{-1}\mathbf{\Sigma}_{(i)}\mathbf{P}_{(i)}^*\mathbf{y}_i, \end{aligned}\tag{3}$$

where $\mathbf{\Sigma}_{(i)}^2 = diag\{\sigma_{i,1}^2,\cdots,\sigma_{i,i-1}^2,\sigma_{i,i+1}^2,\cdots,\sigma_{i,N}^2\}$. The $(N-1)\times(N-1)$ covariance matrix of the MMSE error vector $\Delta\mathbf{h}_{(i)} = \hat{\mathbf{h}}_{(i)} - \mathbf{h}_{(i)}$ is

$$\begin{aligned}\mathbf{K}_{\Delta\mathbf{h}_{(i)}} &= \mathbf{K}_{\mathbf{h}_{(i)}} - \mathbf{K}_{\mathbf{h}_{(i)},\mathbf{y}_i}\mathbf{K}_{\mathbf{y}_i}^{-1}\mathbf{K}_{\mathbf{y}_i,\mathbf{h}_{(i)}} \\ &= \mathbf{\Sigma}_{(i)}^2 - \mathbf{\Sigma}_{(i)}^2\mathbf{P}_{(i)}^*(\mathbf{I}_{n_1} + \mathbf{P}_{(i)}^T\mathbf{\Sigma}_{(i)}^2\mathbf{P}_{(i)}^*)^{-1}\mathbf{P}_{(i)}^T\mathbf{\Sigma}_{(i)}^2 \\ &= \mathbf{\Sigma}_{(i)}\big(\mathbf{I}_{N-1} + \mathbf{\Sigma}_{(i)}\mathbf{P}_{(i)}^*\mathbf{P}_{(i)}^T\mathbf{\Sigma}_{(i)}\big)^{-1}\mathbf{\Sigma}_{(i)}. \end{aligned}\tag{4}$$

Let $\beta_{i,l} = (\mathbf{K}_{\Delta\mathbf{h}_{(i)}})_{l,l}$ be the l-th diagonal element of $\mathbf{K}_{\Delta\mathbf{h}_{(i)}}$, which is the MMSE estimation error variance of the channel between user i and a user $j \neq i$. In Appendix A, we show that as $n_1P_1 \to \infty$, then $\beta_{i,l} \to 0$ for all i and l.

Assume that Eve also uses MMSE for channel estimation. Let $\mathbf{y}_E = vec(\mathbf{Y}_E)$ and $\mathbf{h}_E = vec(\mathbf{H}_E)$. Then (2) becomes

$$\mathbf{y}_E = (\mathbf{P}^T \otimes \mathbf{I}_{N_E})\mathbf{h}_E + \mathbf{n}_E. \tag{5}$$

The MMSE estimate of $\mathbf{h}_E$ (assuming $\mathbf{P}$ is also known to Eve) is

$$\begin{aligned}\hat{\mathbf{h}}_E &= \mathbf{K}_{\mathbf{h}_{E,i},\mathbf{y}_E}\mathbf{K}_{\mathbf{y}_E}^{-1}\mathbf{y}_E \\ &= (\mathbf{\Sigma}_E^2\mathbf{P}^*(\mathbf{I}_{n_1} + \mathbf{P}^T\mathbf{\Sigma}_E^2\mathbf{P}^*)^{-1} \otimes \mathbf{I}_{N_E})\mathbf{y}_E, \end{aligned}\tag{6}$$

where $\mathbf{\Sigma}_E^2 = diag\{\sigma_{E,1}^2,\cdots,\sigma_{E,N}^2\}$. The covariance matrix of $\Delta\mathbf{h}_E = \hat{\mathbf{h}}_E - \mathbf{h}_E$ is

$$\begin{aligned}\mathbf{K}_{\Delta\mathbf{h}_E} &= \mathbf{\Sigma}_E^2 \otimes \mathbf{I}_{N_E} - \mathbf{K}_{\mathbf{h}_E,\mathbf{y}_E}\mathbf{K}_{\mathbf{y}_E}^{-1}\mathbf{K}_{\mathbf{y}_E,\mathbf{h}_E} \\ &= \mathbf{\Sigma}_E^2(\mathbf{I}_{N_E} - \mathbf{P}^*(\mathbf{I}_{n_1} + \mathbf{P}^T\mathbf{\Sigma}_E^2\mathbf{P}^*)^{-1}\mathbf{P}^T\mathbf{\Sigma}_E^2) \otimes \mathbf{I}_{N_E} \\ &= \mathbf{\Sigma}_E(\mathbf{I}_N + \mathbf{\Sigma}_E\mathbf{P}^*\mathbf{P}^T\mathbf{\Sigma}_E)^{-1}\mathbf{\Sigma}_E \otimes \mathbf{I}_{N_E}, \end{aligned}\tag{7}$$

where $\beta_{E,i} = (\mathbf{\Sigma}_E(\mathbf{I}_N + \mathbf{\Sigma}_E\mathbf{P}^*\mathbf{P}^T\mathbf{\Sigma}_E)^{-1}\mathbf{\Sigma}_E)_{i,i}$ is the variance of each elements of $\Delta\mathbf{h}_{E,i}$. It is shown in Appendix A that as $n_1P_1 \to \infty$, we have $\beta_{E,i} \to c_i > 0$ where c_i is invariant to n_1P_1.

B. SNRs at Bob and Eve

In phase 1, ANECE is applied cooperatively by N users as shown previously. We now consider phase 2 where we assume an information transmission between a pair of users. Assume that user i (Alice) transmits the information symbols $x_i(k), k = 1,\cdots,n_2$, to user j (Bob), with transmit power P_2. Then the received signal at Bob is

$$y_j(k) = h_{j,i}x_i(k) + n_j(k) = \hat{h}_{j,i}x_i(k) + \Delta h_{j,i}x_i(k) + n_j(k). \tag{8}$$

The SNR of $y_j(k)$ is $\gamma_b = \frac{(\sigma_{i,j}^2 - \beta_{i,l_j})P_2X_{2,b}}{1+\beta_{i,l_j}P_2X_{1,b}}$ where $X_{1,b} = \frac{|\Delta h_{j,i}|^2}{\beta_{i,l_j}}$ and $X_{2,b} = \frac{|\hat{h}_{j,i}|^2}{\sigma_{i,j}^2 - \beta_{i,l_j}}$ are independent exponentially distributed random variables with unit means.

Similarly, in phase 2, Eve receives

$$\mathbf{y}_{E,i}(k) = \hat{\mathbf{h}}_{E,i}x_i(k) + \Delta\mathbf{h}_{E,i}x_i(k) + \mathbf{n}_E(k). \tag{9}$$

Since Eve knows $\hat{\mathbf{h}}_{E,i}$, we assume that Eve applies maximum ratio combining to achieve a maximum SNR equal to

$$\gamma_e = \frac{\|\hat{\mathbf{h}}_{E,i}\|^2P_2}{1 + \|\frac{\hat{\mathbf{h}}_{E,i}^H}{|\hat{\mathbf{h}}_{E,i}|}\Delta\mathbf{h}_{E,i}\|^2P_2} = \frac{(\sigma_{E,i}^2 - \beta_{E,i})P_2X_{2,e}}{1 + \beta_{E,i}P_2X_{1,e}}, \tag{10}$$

where $X_{1,e} = \|\frac{\hat{\mathbf{h}}_{E,i}^H}{|\hat{\mathbf{h}}_{E,i}|}\frac{\Delta\mathbf{h}_{E,i}}{\sqrt{\beta_{E,i}}}\|^2$ is exponentially distributed with unit mean and $X_{2,e} = \frac{\|\hat{\mathbf{h}}_{E,i}\|^2}{\sigma_{E,i}^2 - \beta_{E,i}}$ follows the Chi-squared distribution with $2N_E$ degrees of freedom (DoF). We will also assume that Eve applies a conventional method to detect the information transmitted by Alice. In other words, Eve treats $\hat{\mathbf{h}}_{E,i}$ as the true channel vector with respect to user i.

C. Achievable Secrecy Rate under FBL

For a finite-block-length (FBL) transmission with $n_2 < \infty$, there are decoding errors at both Bob and Eve. The maximal achievable secrecy rate $R(n_2,\epsilon,\delta)$ with target decoding error probability ϵ at Bob and information leakage δ to Eve can be approximated (according to [11]-[12]) as follows

$$R(n_2,\epsilon,\delta) = \log\left(\frac{1+\gamma_b}{1+\gamma_e}\right) - \sqrt{\frac{V_b}{n_2}}\frac{Q^{-1}(\epsilon)}{\ln 2} - \sqrt{\frac{V_e}{n_2}}\frac{Q^{-1}(\delta)}{\ln 2}, \tag{11}$$

where V_b and V_e are the channel dispersions at Bob and Eve respectively, which can be expressed by $V_x = 1 - (1+\gamma_x)^{-2}$ with $x \in \{b,e\}$. It is typical to choose $\delta \in (0,1/2)$. Let the number of secret information bits transmitted by Alice in every n_2 time slots be n_b. Then, the transmission rate $R(n_2,\epsilon,\delta)$ is set to a constant transmission rate $R^* = \frac{n_b}{n2}$ (details of secrecy coding are discussed in [11]). Therefore, the decoding error ϵ at Bob is no longer constant and subject to random realizations of γ_b and γ_e. Now (11) implies

$$\epsilon = Q\left(\sqrt{\frac{n_2}{V_b}}\left(\ln(\frac{1+\gamma_b}{1+\gamma_e}) - \sqrt{\frac{V_e}{n_2}}Q^{-1}(\delta) - \frac{n_b}{n_2}\ln 2\right)\right), \tag{12}$$

where $\epsilon \triangleq \epsilon(\gamma_b,\gamma_e)$ is now a function of γ_b and γ_e.

Similar to [10] and [13], we consider an averaged achievable secrecy throughput (in bits per channel use) defined by

$$T_s \triangleq \mathbb{E}_{\gamma_b \geq \gamma_e}\left[\frac{n_b}{n_2}(1-\epsilon_{\gamma_b,\gamma_e})\right] \tag{13}$$

where we have excluded the contribution from $\gamma_b < \gamma_e$. Treating γ_b and γ_e as independent random variables, it follows that

$$\begin{aligned} T_s &= \frac{n_b}{n_2}\int_{y=0}^{\infty}\left(\int_{x=y}^{\infty}\big(1-\epsilon(x,y)\big)f_{\gamma_b}(x)\mathrm{d}x\right)f_{\gamma_e}(y)\mathrm{d}y \\ &= \frac{n_b}{n_2}\int_{y=0}^{\infty}\Phi(y)f_{\gamma_e}(y)\mathrm{d}y, \end{aligned} \tag{14}$$

where

$$\Phi(y) = \int_{x=y}^{\infty}\big(1-\epsilon(x,y)\big)f_{\gamma_b}(x)\mathrm{d}x. \tag{15}$$

The rest of the paper focuses on the computational simplification of T_s and the numerical investigation of the tradeoffs among system parameters n_1, n_2, n_b, N, N_E on T_s.

III. Averaged Secrecy Throughput

To compute the averaged secrecy throughput T_s, we need to compute (15) first where $\epsilon(x,y)$ makes the integral an intractable task. As in [9]-[10], we will use the following approximation of $\epsilon(x,y)$:

$$\epsilon(x,y) \approx \begin{cases} 1, & x < x_0 + \frac{1}{2k} \\ \frac{1}{2} + k(x-x_0), & x_0 + \frac{1}{2k} \leq x \leq x_0 - \frac{1}{2k} \\ 0, & x > x_0 - \frac{1}{2k} \end{cases} \tag{16}$$

where x_0 is such that $\epsilon(x_0,y) = 0.5$, i.e., $x_0 = \exp\left(\sqrt{\frac{V_e}{n_2}}Q^{-1}(\delta) + \frac{n_b}{n_2}\ln 2\right)(1+y) - 1$, and $k = \frac{d\epsilon(x,y)}{dx}|_{x=x_0} = -\sqrt{\frac{n_2}{2\pi x_0(x_0+2)}}$. This approximation holds well if $|k|$ is large. Assuming a large $|k|$, it follows from (16) and (15) that

$$\begin{aligned} \Phi(y) &\approx \int_{x_0+\frac{1}{2k}}^{\infty}(1-\epsilon(x,y))f_{\gamma_b}(x)\mathrm{d}x \\ &= 1 - F_{\gamma_b}\left(x_0+\frac{1}{2k}\right) - \int_{x_0+\frac{1}{2k}}^{x_0-\frac{1}{2k}}\left(\frac{1}{2}+k(x-x_0)\right) \\ &\quad \times f_{\gamma_b}(x)\mathrm{d}x \\ &= 1 + k\int_{x_0+\frac{1}{2k}}^{x_0-\frac{1}{2k}} F_{\gamma_b}(x)\mathrm{d}x, \end{aligned} \tag{17}$$

where $F_{\gamma_b}(x)$ is the CDF of γ_b. Since $|k|$ is large, we have $\int_{x_0+\frac{1}{2k}}^{x_0-\frac{1}{2k}} F_{\gamma_b}(x)dx \approx \frac{-1}{k}F_{\gamma_b}(x_0)$ and hence

$$\Phi(y) \approx 1 - F_{\gamma_b}(x_0). \tag{18}$$

where $x_0 \triangleq x_0(y)$ is a function of y.

From Appendix B, we have $F_{\gamma_b}(x) = 1 - \frac{a_j}{a_j+x}e^{-\frac{b_j}{a_j}x}$ where $a_j = \frac{\sigma^2_{j,i}}{\beta_{j,i}} - 1$ and $b_j = \frac{1}{\beta_{j,i}P_2}$. Thus, (18) becomes

$$\Phi(y) \approx \frac{a_j}{a_j + x_0(y)}e^{-\frac{b_j}{a_j}x_0(y)}. \tag{19}$$

From (14), for any $\gamma_1 > 0$, we have

$$T_s = \underbrace{\frac{n_b}{n_2}\int_{y=0}^{\gamma_1}\Phi(y)f_{\gamma_e}(y)\mathrm{d}y}_{T_1} + \underbrace{\frac{n_b}{n_2}\int_{y=\gamma_1}^{\infty}\Phi(y)f_{\gamma_e}(y)\mathrm{d}y}_{T_2}. \tag{20}$$

To compute T_1, we let $g(y) = \Phi(y)f_{\gamma_e}(y)$. Then using the Gaussian-Chebyshev quadrature method [14], it follows that

$$T_1 \approx \frac{n_b}{n_2}\frac{\gamma_1}{2}\sum_{n=1}^{M}\left(\frac{\pi}{M}g\big(\frac{\gamma_1}{2}(t_n+1)\big)\sqrt{1-t_n^2}\right), \tag{21}$$

where $t_n \triangleq \cos(\frac{2n-1}{2M}\pi)$ and the parameter M determines the complexity and accuracy trade-off.

To compute T_2, we simplify $x_0(y)$ by choosing γ_1 sufficiently large such that $V_e = 1-(1+y)^{-2} \approx 1$ for $y \geq \gamma_1$, which implies $x_0(y) \approx \alpha(1+y) - 1$ with constant $\alpha = \exp\left(\frac{Q^{-1}(\delta)}{\sqrt{n_2}} + \ln 2\frac{n_b}{n_2}\right)$. Then, it follows that

$$T_2 \approx \frac{n_b}{n_2}e^{-\frac{b_j}{a_j}(\alpha-1)}\int_{y=\gamma_1}^{\infty}\frac{a_j e^{-\frac{b_j}{a_j}\alpha y}}{\alpha y + \alpha - 1 + a_j}f_{\gamma_e}(y)\mathrm{d}y. \tag{22}$$

To further simplify T_2, we will consider two special cases: Case 1 is for $\beta_{E,i}P_2 \ll 1$, and Case 2 is for $\beta_{E,i}P_2 \gg 1$. Case 1 applies when ANECE is not applied, and Case 2 applies when ANECE is applied. In both cases, we will use $\gamma = \alpha\gamma_1 + \alpha - 1$ to simplify equations.

A. Case 1

In this case, $\beta_{E,i}P_2 \ll 1$ and Eve mainly suffers from the channel background noise. Using $b_x = b_e \to \infty$ in Appendix B, the PDF of γ_e is $f_{\gamma_e}(x) = \frac{\mathrm{d}F_{X_2}(\frac{x}{(\sigma^2_{E,i}-\beta_{E,i})P_2})}{dx} = (\frac{b_e}{a_e})^{N_E}\frac{x^{N_E-1}e^{-\frac{b_e}{a_e}x}}{\Gamma(N_E)}$ where $a_e = \frac{\sigma^2_{E,i}}{\beta_{E,i}} - 1$ and $b_e = \frac{1}{\beta_{E,i}P_2}$. Then the integral in (22) can be expressed in terms of Γ functions and, as shown in Appendix C, (22) becomes

$$\begin{aligned} T_2 \approx a_j\frac{n_b}{n_2}(\frac{b_e}{\alpha a_e})^{N_E}e^{b_j+\frac{b_e}{\alpha a_e}(\alpha-1+a_j)}\sum_{n=0}^{N_E-1}\frac{(\gamma+a_j)^n}{\Gamma(N_E-n)} \\ \times(\alpha\gamma_1)^{N_E-1-n}\Gamma\big(-n, (\frac{b_j}{a_j}+\frac{b_e}{\alpha a_e})(\gamma+a_j)\big). \end{aligned} \tag{23}$$

B. Case 2

In this case, $\beta_{E,i}P_2 \gg 1$ and hence we can ignore the channel background noise at Eve. Thus,

$$\gamma_e = \frac{(\sigma^2_{E,i}-\beta_{E,i})P_2X_{2,e}}{1+\beta_{E,i}P_2X_{1,e}} \approx a_e\frac{X_{2,e}}{X_{1,e}}, \tag{24}$$

and hence $f_{\gamma_e}(x) = \frac{N_E a_e x^{N_E-1}}{(a_e+x)^{N_E+1}}$ (which also follows from Appendix B). Then T_2 in (22) becomes

$$T_2 \approx \frac{n_b}{n_2}\frac{a_j a_e}{\alpha} N_E \int_{y=\gamma_1}^{\infty} \frac{e^{-\frac{b_j}{a_j}(\alpha y+\alpha-1)} y^{N_E-1}}{(y+\frac{\alpha-1+a_j}{\alpha})(a_e+y)^{N_E+1}} \mathrm{d}y$$
$$= \frac{n_b}{n_2}\frac{a_j a_e e^{-\frac{b_j}{a_j}(\alpha-1)}}{\alpha-1+a_j} N_E \Bigg[\int_{y=\gamma_1}^{\infty} \frac{e^{-\frac{b_j}{a_j}\alpha y} y^{N_E-1}}{(a_e+y)^{N_E+1}} \mathrm{d}y$$
$$- \int_{y=\gamma_1}^{\infty} \frac{e^{-\frac{b_j}{a_j}\alpha y} y^{N_E}}{(y+\frac{\alpha-1+a_j}{\alpha})(a_e+y)^{N_E+1}} \mathrm{d}y \Bigg], \quad (25)$$

after applying the change of variable $x = \frac{1}{y}$ in (25), we get

$$T_2 = \frac{n_b}{n_2}\frac{a_j a_e e^{-\frac{b_j}{a_j}(\alpha-1)}}{\alpha-1+a_j} N_E \Bigg[\underbrace{\int_{y=\gamma_1}^{\infty} \frac{e^{-\frac{b_j}{a_j}\alpha y} y^{N_E-1}}{(a_e+y)^{N_E+1}} \mathrm{d}y}_{\Omega(\gamma_1)}$$
$$- \int_{x=0}^{\frac{1}{\gamma_1}} \underbrace{\frac{e^{-\frac{b_j}{a_j}\frac{\alpha}{x}}}{(1+\frac{\alpha-1+a_j}{\alpha}x)(1+a_e x)^{N_E+1}}}_{h(x)} \mathrm{d}x \Bigg]$$
$$\approx \frac{n_b}{n_2}\frac{a_j a_e e^{-\frac{b_j}{a_j}(\alpha-1)}}{\alpha-1+a_j} N_E \Omega(\gamma_1) - \frac{n_b}{n_2}\frac{a_j a_e e^{-\frac{b_j}{a_j}(\alpha-1)}}{\alpha-1+a_j}$$
$$\times \frac{N_E}{2\gamma_1} \sum_{n=1}^{M} \left(\frac{\pi}{M} h\Big(\frac{1}{2\gamma_1}(t_n+1)\Big)\sqrt{1-t_n^2} \right), \quad (26)$$

where we have applied the Gaussian-Chebyshev quadrature method on the function denoted as $h(x)$. Furthermore, $\Omega(\gamma_1)$ in (26) is shown in Appendix D to be

$$\Omega(\gamma_1) = e^{-\frac{b_j}{a_j}\alpha\gamma_1}\Gamma(N_E) \sum_{n=0}^{N_E-1} \frac{1}{\Gamma(N_E-n)} \frac{\gamma_1^{N_E-1-n}}{(a_e+\gamma_1)^{N_E-n}}$$
$$\times U\left(n+1, n+1-N_E, \frac{b_j}{a_j}\alpha(a_e+\gamma_1)\right). \quad (27)$$

IV. Numerical Results

In this section, we show numerical results of the averaged secrecy throughput T_s of secret information transmission from user 1 to user 2 among $N \geq 2$ cooperative single-antenna full-duplex users for which $\sigma_{i,j} = 1$ for all i and $j \neq i$. Unless otherwise specified, we use $P_1 = P_2 = 25$dB, $\delta = 0.001$, $N_E = 4$, $\sigma_E = 1$, $n_1 = 4$, $n_2 = 300$, and $n_b = 200$. To compute T_1 and T_2 in (20), we use $\gamma_1 = 10$ and $M = 16$. To verify our theoretical results (TR), we also conducted a 10^4-run Monte Carlo (MC) simulation to compute the expectation in (13).

In Fig. 1, we show T_s versus n_2 for different N_E, which also compares the cases of "with ANECE" (under ideal full-duplex) and "without ANECE". The case of "with ANECE" is based on $N = 4$ cooperative users in phase 1, but only user 1 transmits secret information to user 2 in phase 2. For the case of "without ANECE", only user 1 sends a pilot in phase 1 which allows both user 2 and Eve to obtain consistent channel estimates. We see a significant gap of T_s between the

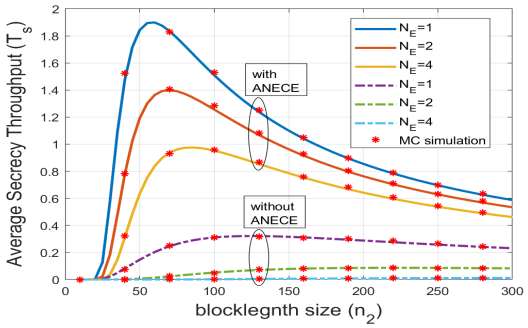

Fig. 1. T_s versus n_2 for $N_E = 1, 2, 4$ and $N = 4$.

cases of "with ANECE" and "without ANECE". We also see that as n_2 increases, T_s increases initially and then decreases.

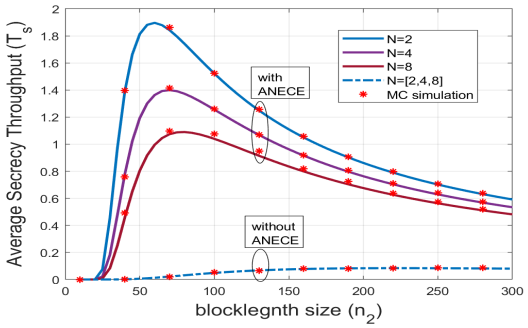

Fig. 2. T_s versus n_2 for $N_E = 2$ and $N = 2, 4, 8$.

In Fig. 2, we show T_s versus n_2 for $N_E = 2$ and $N = 2, 4, 8$. We observe that with ANECE, the averaged secrecy throughput T_s from user 1 to user 2 is maximum when only users 1 and 2 (i.e., $N = 2$) perform ANECE cooperatively. However, we should note that using $N > 2$ cooperative users for ANECE, multiple pairs of users can then transmit secret information to each other without the need for additional phases of channel training. The sum of pair-wise secrecy throughput of all users can scale up linearly with the number of pairs if Eve only applies conventional methods for channel estimation and information detection.

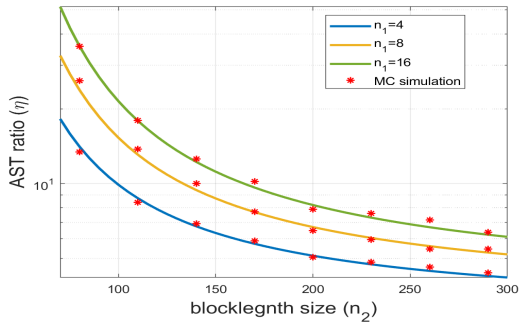

Fig. 3. η vs n_2 for $n_1 = 4, 8, 16$, $N_E = 2$ and $N = 4$.

In Fig. 3, we present the ratio $\eta \triangleq \frac{T_s^{(withANECE)}}{T_s^{(withoutANECE)}}$ versus n_2 for $n_1 = 4, 8, 16$, $N_E = 2$ and $N = 4$. We observe that η is an increasing function of n_1, and $\eta > 1$ for all n_1 and n_2.

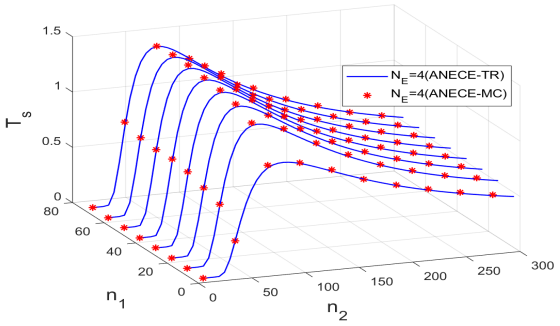

Fig. 4. T_s vs n_1 and n_2 for the ANECE-assisted case.

In Fig. 4, we show T_s vs n_1 and n_2 for the ANECE-assisted case with $N = 4$, $P_1 = P_2 = 25$dB and $N_E = 4$. We see that T_s is an increasing function of n_1. Fig. 5 depicts the ANECE-assisted T_s versus n_2 and n_b (the number of secret bits transmitted per block). Here we also observe the quasi-concave nature of T_s with respect to n_2 for each fixed n_b. Thus, the theoretical results can be used to accurately find the optimal n_2. Furthermore, the optimal n_2 increases with n_b.

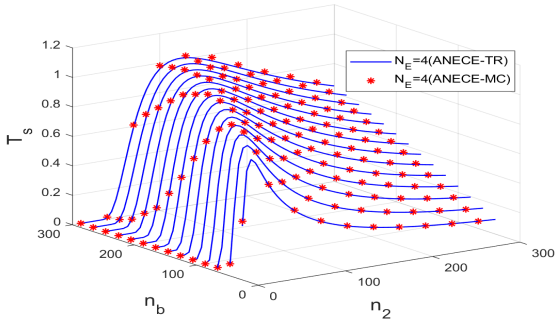

Fig. 5. T_s vs n_2 and n_b for $N = 4$ and $N_E = 4$.

V. Conclusion

We have analysed AST of ANECE assisted transmission between single-antenna full-duplex devices against an eavesdropper with multiple antennas. The resulting expressions for AST are easy to compute and consistent with the results from costly Monte Carlo simulations. This analysis reveals a large gain of secrecy achievable from ANECE. Furthermore, this analysis is done in the context of finite blocklength transmission, which is important for latency sensitive applications.

Appendix A
Properties of $\beta_{i,l}$ and $\beta_{E,i}$

Let the eigenvalue decomposition (EVD) of $\mathbf{\Sigma}_{(i)}\mathbf{P}^*_{(i)}\mathbf{P}^T_{(i)}\mathbf{\Sigma}_{(i)}$ with descending eigenvalues be $\sum_{k=1}^{N-1}\lambda_{i,k}\mathbf{u}_{i,k}\mathbf{u}_{i,k}^H = \mathbf{U}_i\mathbf{\Lambda}_i\mathbf{U}_i^H$. It follows from (4) that

$$\mathbf{K}_{\Delta\mathbf{h}_{(i)}} = \mathbf{\Sigma}_{(i)}\mathbf{U}_i(\mathbf{I}+\mathbf{\Lambda}_i)^{-1}\mathbf{U}_i^H\mathbf{\Sigma}_{(i)} = \sum_{k=1}^{N-1}\frac{\mathbf{v}_{i,k}\mathbf{v}_{i,k}^H}{1+\lambda_{i,k}}, \quad (28)$$

where $\mathbf{v}_{i,k} = \mathbf{\Sigma}_{(i)}\mathbf{u}_{i,k}$. From (28) we get

$$\beta_{i,l} = (\mathbf{K}_{\Delta\mathbf{h}_{(i)}})_{l,l} = \sum_{k=1}^{N-1}\frac{(\mathbf{v}_{i,k}\mathbf{v}_{i,k}^H)_{l,l}}{1+\lambda_{i,k}}. \quad (29)$$

Clearly, $\beta_{i,l} \to 0$ if $\min_k \lambda_{i,k} = \lambda_{i,N-1} \to \infty$.

As discussed in Section II, the ANECE pilot matrix $\mathbf{P} = \mathbf{DQV}$, where $\mathbf{Q}$ is the $N \times (N-1)$ submatrix of $\mathbf{F}$, the DFT matrix of size N, with entries $\exp(-j2\pi mn/N)$. Then, to get a constant row norm of $\sqrt{P_1 n_1}$, $\mathbf{D}$ must have constant diagonal entries equal to $d = \sqrt{P_1 n_1/(N-1)}$.

Let $\mathbf{Q}_i$ denote the matrix obtained by dropping the i-th row of $\mathbf{Q}$. Then $\mathbf{P}_{(i)} = d\mathbf{Q}_i\mathbf{V}$. By the interlacing property of eigenvalues, we know that $N-2$ of the $N-1$ eigenvalues of $\mathbf{Q}_i\mathbf{Q}_i^H$ are equal to N. It can be verified that the diagonal elements of $\mathbf{Q}_i\mathbf{Q}_i^H$ are all equal to $N-1$. Thus, from the trace property it follows that the smallest eigenvalue of $\mathbf{Q}_i\mathbf{Q}_i^H$ is $(N-1)^2 - N(N-2) = 1$. Thus the matrix $\mathbf{P}_{(i)}\mathbf{P}_{(i)}^H = d^2\mathbf{Q}_i\mathbf{Q}_i^H$ has full rank; its smallest eigenvalue is d^2. Since the matrix $\mathbf{\Sigma}_{(i)}$ has full rank, it follows that $\lambda_{i,N-1} > 0$, and hence this eigenvalue goes to infinity as $P_1 n_1 \to \infty$.

Similarly, let the EVD of the $N \times N$ matrix $\mathbf{\Sigma}_E\mathbf{P}^*\mathbf{P}^T\mathbf{\Sigma}_E$ with descending eigenvalues be $\sum_{k=1}^{N}\lambda_{E,k}\mathbf{u}_{E,k}\mathbf{u}_{E,k}^H = \mathbf{U}_E\mathbf{\Lambda}_E\mathbf{U}_E^H$ where $\lambda_{E,N} = 0$. Let $\mathbf{v}_{E,k} = \mathbf{\Sigma}_E\mathbf{u}_{E,k}$. Then, it follows from (7) that

$$\begin{aligned}\mathbf{K}_{\Delta\mathbf{h}_E} &= \left(\sum_{k=1}^{N-1}\frac{\mathbf{v}_{E,k}\mathbf{v}_{E,k}^H}{1+\lambda_{E,k}} + \mathbf{v}_{E,N}\mathbf{v}_{E,N}^H\right)\otimes\mathbf{I}_{N_E} \\ &\geq (\mathbf{v}_{E,N}\mathbf{v}_{E,N}^H)\otimes\mathbf{I}_{N_E}, \end{aligned} \quad (30)$$

where the lower bound is achieved when $n_1 P_1 \to \infty$. Consequently, $\beta_{E,i} = (\sum_{j=1}^{N-1}\frac{\mathbf{v}_{E,j}\mathbf{v}_{E,j}^H}{1+\lambda_{E,j}} + \mathbf{v}_{E,N}\mathbf{v}_{E,N}^H)_{i,i} \geq (\mathbf{v}_{E,N}\mathbf{v}_{E,N}^H)_{i,i} \triangleq c_i$, which is positive.

Appendix B
CDFs and PDFs of γ_e and γ_b

SNRs γ_e and γ_b, defined in Sec. II-B, can be written as

$$\gamma_x = \frac{a_x X_2}{b_x + X_1}, \quad (31)$$

where X_1 and X_2 are independent, X_1 is exponentially distributed with unit mean, and X_2 is Chi-square distributed with DoF equal to $2N_x$. Then the CDF of γ_x is

$$\begin{aligned} F_{\gamma_x}(z) &= P\big[X_1 > \frac{a_x X_2}{z} - b_x\big] = 1 - P\left[X_1 < \frac{a_x X_2}{z} - b_x\right] \\ &= 1 - \int_{x=\frac{b_x}{a_x}z}^{\infty}\left(1 - e^{-(\frac{a_x}{z}x - b_x)}\right) f_{X_2}(x)\mathrm{d}x \\ &= F_{X_2}(\frac{b_x}{a_x}z) + \frac{e^{b_x}}{\Gamma(N_x)}\int_{x=\frac{b_x}{a_x}z}^{\infty} e^{-x(\frac{a_x}{z}+1)}x^{N_x-1}\mathrm{d}x \\ &= F_{X_2}(\frac{b_x}{a_x}z) + \frac{e^{b_x}\int_{y=\frac{b_x}{a_x}z+b_x}^{\infty} e^{-y}y^{N_x-1}\mathrm{d}y}{(\frac{a_x}{z}+1)^{N_x}\Gamma(N_x)} \\ &= F_{X_2}(\frac{b_x}{a_x}z) + \frac{e^{b_x}\left(1 - F_{X_2}(\frac{b_x}{a_x}z + b_x)\right)}{(\frac{a_x}{z}+1)^{N_x}}, \end{aligned} \quad (32)$$

where $F_{X_2}(\frac{b_x}{a_x}z) = 1 - \frac{\Gamma(N_x, \frac{b_x}{a_x}z)}{\Gamma(N_x)}$, and the second term in the last expression of (32) is zero if $b_x \to \infty$. Then the PDF of γ_x is

$$\begin{aligned} f_{\gamma_x}(z) &= \tfrac{b_x}{a_x} f_{X_2}(\tfrac{b_x}{a_x}z) + \tfrac{e^{b_x}}{\Gamma(N_x)}\big[0 - \tfrac{b_x}{a_x}e^{-(\frac{b_x}{a_x}z)(\frac{a_x}{z}+1)} \\ &\quad \times (\tfrac{b_x}{a_x}z)^{N_x-1} + \tfrac{a_x}{z^2}\textstyle\int_{x=\frac{b_x}{a_x}z}^{\infty} e^{-x(\frac{a_x}{z}+1)}x^{N_x}dx\big] \\ &= \tfrac{a_x e^{b_x}}{\Gamma(N_x)} \tfrac{z^{N_x-1}}{(z+a_x)^{N_x+1}}\Gamma(N_x+1, \tfrac{b_x}{a_x}z + b_x). \quad (33) \end{aligned}$$

For γ_e, $N_x = N_E$, $a_x = a_e = \frac{\sigma_{E,i}^2}{\beta_{E,i}} - 1$ and $b_x = b_e = \frac{1}{\beta_{E,i}P_2}$. For γ_b, $N_x = 1$, $a_x = a_j = \frac{\sigma_{j,i}^2}{\beta_{j,i}} - 1$ and $b_x = b_j = \frac{1}{\beta_{j,i}P_2}$.

Appendix C
Proof of (23)

$$\begin{aligned} T_2 &= a_j \frac{n_b}{n_2} \frac{(\frac{b_e}{a_e})^{N_E} e^{-\frac{b_j}{a_j}(\alpha-1)}}{\Gamma(N_E)} \int_{y=\gamma_1}^{\infty} \frac{e^{-\frac{b_j}{a_j}\alpha y - \frac{b_e}{a_e}y} y^{N_E-1}}{\alpha y + \alpha - 1 + a_j} \mathrm{d}y \\ &\overset{(a)}{=} a_j \frac{n_b}{n_2} \frac{(\frac{b_e}{\alpha a_e})^{N_E} e^{-\frac{b_j}{a_j}\gamma - \frac{b_e}{a_e}\gamma_1}}{\Gamma(N_E)} \\ &\quad \times \int_{z=0}^{\infty} \frac{(\alpha\gamma_1 + z)^{N_E-1}}{z + \gamma + a_j} e^{-(\frac{b_j}{a_j} + \frac{b_e}{\alpha a_e})z} \mathrm{d}z \\ &= a_j \frac{n_b}{n_2} \frac{(\frac{b_e}{\alpha a_e})^{N_E} e^{-\frac{b_j}{a_j}\gamma - \frac{b_e}{a_e}\gamma_1}}{\Gamma(N_E)} \sum_{n=0}^{N_E-1} \binom{N_E-1}{n} \\ &\quad \times (\alpha\gamma_1)^{N_E-1-n} \int_{z=0}^{\infty} \frac{z^n}{z + \gamma + a_j} e^{-(\frac{b_j}{a_j} + \frac{b_e}{\alpha a_e})z} \mathrm{d}z \\ &\overset{(b)}{=} a_j \frac{n_b}{n_2} \frac{(\frac{b_e}{\alpha a_e})^{N_E} e^{-\frac{b_j}{a_j}\gamma - \frac{b_e}{a_e}\gamma_1}}{\Gamma(N_E)} \sum_{n=0}^{N_E-1} \binom{N_E-1}{n} \\ &\quad \times (\alpha\gamma_1)^{N_E-1-n} (\gamma + a_j)^n e^{(\frac{b_j}{a_j} + \frac{b_e}{\alpha a_e})(\gamma + a_j)} \\ &\quad \times \Gamma(n+1)\Gamma\big(-n, (\frac{b_j}{a_j} + \frac{b_e}{\alpha a_e})(\gamma + a_j)\big) \\ &= a_j \frac{n_b}{n_2} (\frac{b_e}{\alpha a_e})^{N_E} e^{b_j + \frac{b_e}{\alpha a_e}(\alpha - 1 + a_j)} \sum_{n=0}^{N_E-1} \frac{(\gamma + a_j)^n}{\Gamma(N_E - n)} \\ &\quad \times (\alpha\gamma_1)^{N_E-1-n} \Gamma\big(-n, (\frac{b_j}{a_j} + \frac{b_e}{\alpha a_e})(\gamma + a_j)\big), \quad (34) \end{aligned}$$

where step $\overset{(a)}{=}$ follows from the variable change $z = \alpha(y - \gamma_1)$, and step $\overset{(b)}{=}$ follows from the equation (3.383.10) in [15].

Appendix D
Proof of (27)

$$\begin{aligned} \Omega(\gamma_1) &= \int_{y=\gamma_1}^{\infty} \frac{e^{-\frac{b_j}{a_j}\alpha y} y^{N_E-1}}{(a_e + y)^{N_E+1}} \mathrm{d}y \\ &\overset{(a)}{=} \int_{x=0}^{\infty} \frac{e^{-\frac{b_j}{a_j}\alpha(\gamma_1 + x)} (\gamma_1 + x)^{N_E-1}}{(a_e + \gamma_1 + x)^{N_E+1}} \mathrm{d}x \\ &= \frac{\gamma_1^{N_E-1} e^{-\frac{b_j}{a_j}\alpha\gamma_1}}{(a_e + \gamma_1)^{N_E+1}} \int_{x=0}^{\infty} \frac{e^{-\frac{b_j}{a_j}\alpha x} (1 + \frac{x}{\gamma_1})^{N_E-1}}{(1 + \frac{x}{a_e + \gamma_1})^{N_E+1}} \mathrm{d}x \\ &\overset{(b)}{=} \frac{\gamma_1^{N_E-1} e^{-\frac{b_j}{a_j}\alpha\gamma_1}}{(a_e + \gamma_1)^{N_E}} \sum_{n=0}^{N_E-1} \binom{N_E-1}{n} \frac{(a_e + \gamma_1)^n}{\gamma_1^n} \\ &\quad \times \int_{z=0}^{\infty} \frac{e^{-\frac{b_j}{a_j}\alpha(a_e + \gamma_1)z} z^n}{(1+z)^{N_E+1}} \mathrm{d}z, \quad (35) \end{aligned}$$

where steps $\overset{(a)}{=}$ and $\overset{(b)}{=}$ follow from the changes of variables $x = y - \gamma_1$ and $z = \frac{x}{a_e + \gamma_1}$ respectively. After applying $\int_{z=0}^{\infty} \frac{t^{a-1}e^{-zt}}{(1+t)^{a+1-b}} \mathrm{d}t = \Gamma(a)U(a, b, z)$ from [15] in (35), we get

$$\begin{aligned} \Omega(\gamma_1) &= e^{-\frac{b_j}{a_j}\alpha\gamma_1} \Gamma(N_E) \sum_{n=0}^{N_E-1} \frac{1}{\Gamma(N_E - n)} \frac{\gamma_1^{N_E-1-n}}{(a_e + \gamma_1)^{N_E-n}} \\ &\quad \times U(n+1, n+1-N_E, \frac{b_j}{a_j}\alpha(a_e + \gamma_1)). \quad (36) \end{aligned}$$

References

[1] Y. Hua, "Advanced properties of full-duplex radio for securing wireless network," IEEE Trans. on Signal Processing, Vol. 67, No. 1, pp. 120-135, Jan. 2019.

[2] R. Sohrabi, Q. Zhu, and Y. Hua, "Secrecy analyses of a full-duplex MIMOME network", IEEE Trans. Signal Processing, Vol. 67, No. 23, pp. 5968-5982, Dec. 2019.

[3] Q. Zhu, S. Wu, and Y. Hua, "Optimal pilots for anti-eavesdropping channel estimation," IEEE Trans. on Signal Processing, Vol. 68, pp. 2629-2644, 2020.

[4] G. Durisi, T. Koch, and P. Popovski, "Toward massive, ultrareliable, and low-latency wireless communication with short packets," Proc. IEEE, vol. 104, no. 9, pp. 1711-1726, Sep. 2016.

[5] R. Chen, C. Li, S. Yan, R. Malaney, and J. Yuan, "Physical layer security for ultra-reliable and low-latency communications," IEEE Trans. Wireless Commun., vol. 26, no. 5, pp. 6-11, 2019.

[6] T. Zheng, H. Wang, D. W. K. Ng and J. Yuan, "Physical-Layer Security in the Finite Blocklength Regime over Fading Channels," in IEEE Trans. on Wireless Commun., Vol. 19, No. 5, pp. 3405-3420, 2020.

[7] N. Ari, N. Thomos and L. Musavian, "Average Secrecy Throughput Analysis with Multiple Eavesdroppers in the Finite Blocklength," 2020 IEEE 31st Annual International Symposium on Personal, Indoor and Mobile Radio Communications, London, UK, pp. 1-5,2020.

[8] H. Wang, Q. Yang, Z. Ding, and H. V. Poor, "Secure short-packet communications for mission-critical IoT applications," IEEE Trans. Wireless Commun., vol. 18, no. 5, pp. 2565-2578, 2019.

[9] B. Makki, T. Svensson, and M. Zorzi, "Finite block-length analysis of the incremental redundancy HARQ," IEEE Wireless Commun. Lett., vol. 3, no. 5, pp. 529-532, 2014.

[10] B. Makki, T. Svensson, and M. Zorzi, "Wireless energy and information transmission using feedback: Infinite and finite block-length analysis," IEEE Trans. Commun., vol. 64, no. 12, pp. 5304-5318, Dec. 2016.

[11] W. Yang, R. F. Schaefer, and H. V. Poor, "Finite-blocklength bounds for wiretap channels," in Proc. IEEE Int. Symp. Inf. Theory (ISIT), Barcelona, Spain, Jul. 2016, pp. 3087-3091.

[12] Y. Polyanskiy, H. V. Poor, and S. Verdu, "Channel coding rate in the finite blocklength regime," IEEE Trans. Inf. Theory, vol. 56, no. 5, pp. 2307-2359, May 2010.

[13] P. Mary, J. Gorce, A. Unsal and H. V. Poor, "Finite Blocklength Information Theory: What Is the Practical Impact on Wireless Communications?," in Proc. IEEE Globecom Workshops, Washington, DC, pp. 1-6, 2016.

[14] F. B. Hildebrand, "Introduction to Numerical Analysis," 2nd ed. Mineola, NY, USA: Dover, 1987.

[15] I. S. Gradshteyn and I. M. Ryzhik, "Table of Integrals, Series, and Products," 7th ed. New York, NY, USA: Academic, 2007.